Potential Performance of SiC and GaN Based Metal Semiconductor Field Effect Transistors

H. Arabshahi*
Department of Physics, Ferdowsi University of Mashhad,
P.O. Box 91775-1436, Mashhad, Iran
(Received on 23 July, 2008)

A Monte Carlo simulation has been used to model steady-state electron transport in SiC and GaN field effect transistor. The simulated device geometries and doping are matched to the nominal parameters described for the experimental structures as closely as possible. Simulations of SiC MESFETs of lengths 2, 2.6 and 3.2 μm have been carried out and compared these results with those on GaN MESFETs of the same dimensions. The direct current *IV* characteristics of the two materials were found to be similar, though the GaN characteristics were on the whole superior, reaching their operating point at higher drain voltages and possessing higher gains. However, oscillations in the drain current caused by changes in drain voltage in the GaN devices were not present to the same degree in the SiC devices. This difference is caused partially by the onset of the negative differential regime in SiC at a higher electric field than in GaN but the primary cause is the longer ballistic transport times in SiC. This suggests that GaN MESFETs may prove to have superior frequency response characteristics than SiC MESFETs.

Keywords: Ballistic transport; frequency response; Steady-state; Drain current

1. INTRODUCTION

SiC and GaN are wide bandgap semiconductors, and therefore have a high breakdown field and low thermal generation rate. These properties combined with good thermal conductivity and stability make them as an attractive material for high power, high temperature and radiation harsh environment electronic devices. Monte Carlo simulations pridict a peak electron velocity of 3×10^5 ms^{-1} and 2.3×10^5 ms^{-1} for SiC and GaN materials, respectively [1-2]. This makes possible high frequency operation devices.
The metal semiconductor field effect transistor (MESFET) is one of the most favoured devices in the construction of large scale integrated circuits because of its simplicity of construction, the comparative lack of dopant diffusion problems and the resultant high packing densities possible. Whilst the preferred semiconductor is still silicon, industry is now tooling up for wide band gap semiconductors like GaN or SiC production, which offers high electron mobility and hence the prospect of greater frequency operating rates. Their direct bandgap furthermore allows easier integration with optical devices. For this reason GaN MESFETs have received much attention in the literature, particularly with respect to their simulation [3-4] in an attempt to understand the basic principles of their operation. Monte Carlo methods have been used to a great extent in this effort because they allow an essentially exact solution of the Boltzmann transport equation and are subject only to statistical errors, unlike drift diffusion models which cannot accurately treat the hot-electron effects that are present to a high degree in GaN devices [5]. SiC offers the prospect of mobilities comparable to GaN and is increasingly being developed for the construction of optical switches. Other authors have also pointed out the potential importance of SiC and a few simple devices have been simulated [6]. This paper presents the results of a Monte Carlo simulation which is used to model electron transport in wurtzite GaN and SiC MESFETs including different tansistor lengths at room temperature. The simulations have been carried out using a non-parabolic ellipsoidal valley model to describe transport in the conduction band.
This article is organised as follows. Details of the device fabrication model which is used in the simulated device are presented in section 2, and results for simulation carried out on GaN and SiC MESFETs are interpreted in section 3.

*Electronic address: arabshahi@um.ac.ir

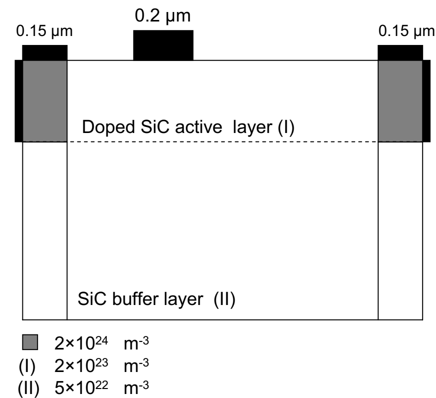

FIG. 1: The two-dimensional model of SiC/GaN MESFET. The modelled structure is divided into three regions, as indicated. Electron particles are initially distributed keeping all regions charge neutral. The location of the source and the drain implants and the top and back buffer layer are marked.

2. MODEL DETAILS

The Monte Carlo method may be used to simulate the motion of charge carriers through a semiconductor device by following the progress of several tens of thousands of test or representative superparticles. These particles are propagated classically between collisions according to their velocity, effective mass and the prevailing field. The selection of quantities such as the propagation time of a particle between scattering events or the mechanism by which the particle is to be scattered is done by generating a random number and using the number to choose the required quantity from predetermined tables of

Bulk material parameters	SiC	GaN			
Density ρ (kgm^{-3})	3200	6150			
Longitudinal sound velocity v_s (ms^{-1})	1373	4330			
Low-frequency dielectric constant ε_s	9.7	9.5			
High-frequency dielectric constant ε_∞	6.5	5.35			
Acoustic deformation potential D (eV)	15	8.3			
Polar optical phonon energy $\hbar\omega_{op}$ (meV)	120	99			
Bandgap E_g (meV)	3.2	3.5			
Valley dependent parameters	Γ_1	U	Γ_3	M	K
Effective mass (m^*/m_0):					
SiC	0.28	0.39	0.6	0.57	0.54
GaN	0.2	0.4	0.6	0.57	0.3
Nonparabolicity (eV^{-1}):					
SiC	0.32	0.5	0.029	0.0	0.03
GaN	0.189	0.065	0.029	0.0	0.7
Valley separation from Γ_1-valley (eV):					
SiC	0.0	0.61	1.3	0.9	0.67
GaN	0.0	2	1.9	3	3.1
Number of equvalet valley	1	6	1	3	2

Table 1. Important parameters used in our simulations for wurtzite phase SiC and GaN materials.

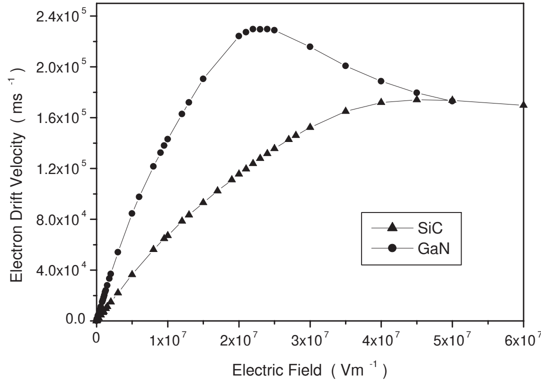

FIG. 2: Relationships between electron drift velocity and electric field for GaN (circles) and SiC (triangles) found using the parameters of table 1.

probabilities for each process. Thorough discussions of the Monte Carlo method are given by Fawcett *et. al* [7] and Jacoboni *et. al* [8], and for a review see Moglestue *et. al* [9].

In this work, the two lowest energy conduction bands of the empirical pseudopotential band structure for wurtzite phase of SiC and GaN are chosen as a basis of an analytical multivalley conduction band model [10-13]. The pseudopotential band structure shows the conduction band minimum to be located at the Γ point (Γ_1), and lowest energy conduction band satellite valleys to occur at the U point (located about two thirds of the way between the L and M symmetry points). Higher conduction band valleys are located at the Γ point (Γ_3), at the M point, and at the K point. In our Monte Carlo simulation, the two different Γ valleys, the six equivalent U valleys, the three equivalent M valleys, and the two equivalent K valleys, are represented by ellipsoidal, nonparabolic dispersion relationships of the following form [8-9]

$$E(\mathbf{k})[1+\alpha_i E(\mathbf{k})] = \frac{\hbar^2}{2}\left[\frac{k_x^2+k_y^2}{m_\perp^*}+\frac{k_z^2}{m_\parallel^*}\right] \qquad (1)$$

where $m_\perp^*$ and $m_\parallel^*$ are the transverse and longitudinal effective masses at the band edge and α_i is the non-parabolicity coefficient of the i-th valley. The material and valley parameters necessary for calculating the scattering probabilities used in the present Monte Carlo simulation are listed in table 1.

Electron particles in the employed ensemble Monte Carlo simulation occupy non-parabolic ellipsoidal valleys in reciprocal space, and obey Boltzmann statistics. Herring-vogt transformations are used to map carrier momenta into spherical valleys when particles are drifted, scattered or cross heterojunctions (where care has been taken to ensure that the crystal momentum in the plane of the junction is conserved across the interface). The electric field equations are solved self-consistently with the electron transport using a finite difference method [14], and the device grid potentials are updated at each ensemble drift timestep (1 femtosecond). Electrons in the bulk are scattered by ionised impurities and by bulk acoustic and non-polar optical phonon modes. Intervalley scattering by the absorption and emission of long wavelength acoustic and optic phonons have also been considered in the model. As described in detail [8-9], model devices are built up as a series of joined rectangular regions, with the electric field cell sizes matched along the join between each region. Each region can consist of multiple layers of different alloy composition and doping/compensation density.

The SiC/GaN MESFET can be described simply by three regions (figure 1), representing source and drain doping implants and a central region containing the supply layers. The field cell

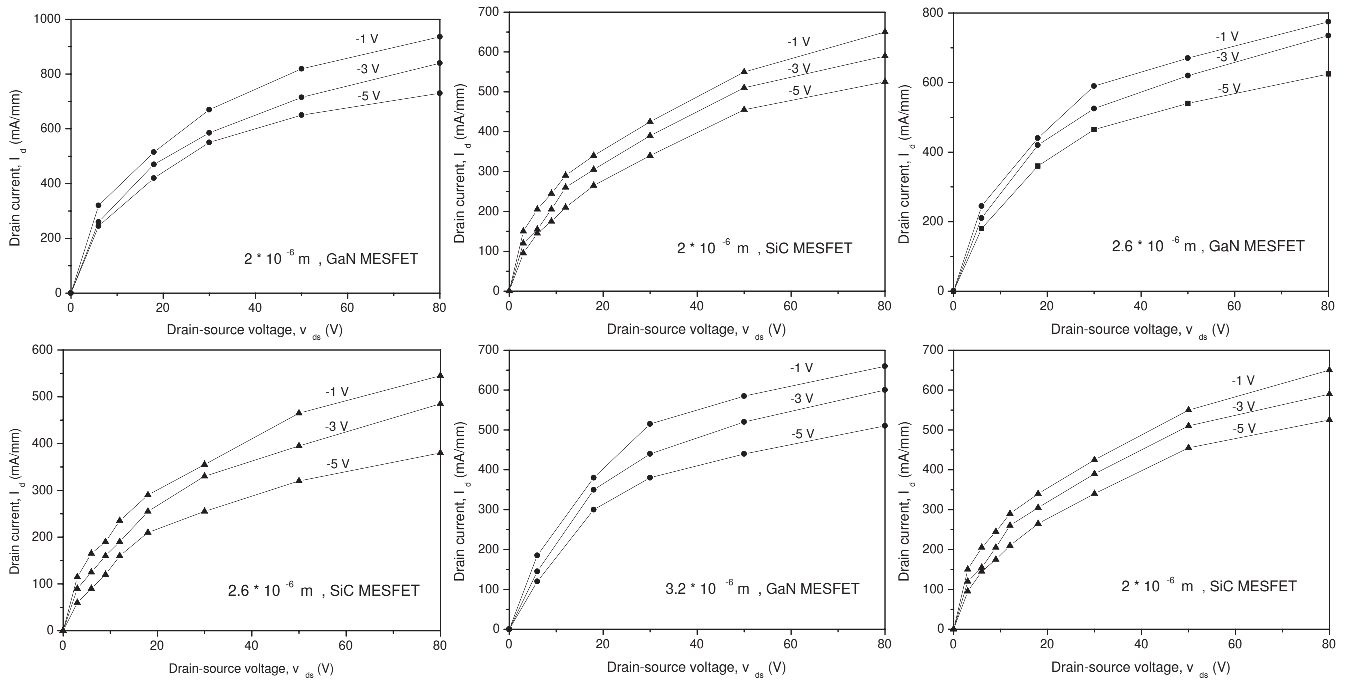

FIG. 3: Static *IV* characteristics for GaN and SiC MESFETs for effective gate voltages of -1 V to -5 V and for different device length.

size used for the central region is 30 nm^2 (horizontal$\times$vertical), but that in the high doped source and drain implants is finer (10 nm^2). Simulations of steady current characteristics have been carried out using 20000 electron paticles.
Figure 1 shows a schematic of the modelled SiC/GaN MESFET. The overall device length is 2μm in the x-direction and the device has a 0.2μm gate length and 0.15μm source and drain length. The source and drain have ohmic contacts and gate is in Schottky contact in 1 eV to represent the contact potential at Au/Pt. The source and drain regions are doped to 2×10^{24} m^{-3} electron concentration and the top and down buffer layers are doped to 2×10^{23} m^{-3} and 5×10^{22} m^{-3} electron concentration, respectively.
The drain current is obtained by counting the net charge flow through the drain contact. For the static *IV* characteristics, the simulation was continued until the current converged to a value with an error of less than 1 A in two successive 10 ps intervals. The relationships between field and drift velocity obtained for each material are shown in figure 2, where they are seen to compare well with [15-16].

3. RESULTS AND DISCUSSION

The computed $I_{ds}(V_{ds}, V_{gs})$ characteristics are presented in figure 3 for both GaN and SiC MESFET. The obtained characteristics are almost identical in shape. For both structures, one observes that the output conductance is quite large and that the device is not completely pinched-off even at large negative gate bias. These two effects are mainly due to short channel effects and strong electron injection in the buffer layer. A part of the drain current flows through the buffer and increases with increasing drain voltage. This effect is more important at high V_{gs}, e.g. at V_{gs}=-13 V, the whole drain current flows entirely through the buffer. This is due to the low conduction band discontinuity at the interface between GaN/SiC and their buffer layers. Nevertheless, for both structures, high drain current densities are obtained, confirming that GaN or SiC MESFETs are good candidates for high power applications. Moreover, due to the better electronic transport properties in GaN, the GaN based MESFET exhibits a 70% higher drain current density as compared with the SiC MESFET.
The effect of device length on output drain current have also been studied in figure 3. It is apparent from this figure, that higher drain current are reached as the device length is reduced as a result of the increase in longitudinal electric field and velocity overshoot effects. It follows that the electron transit time

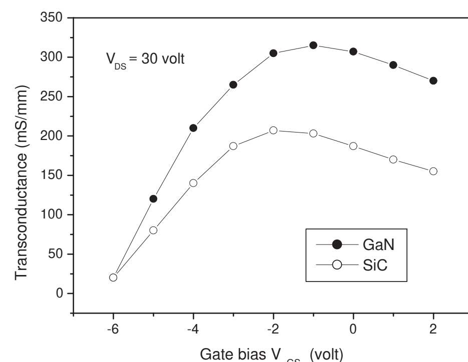

FIG. 4: Transconductance as a function of gate bias. Comparison of GaN and SiC MESFET.

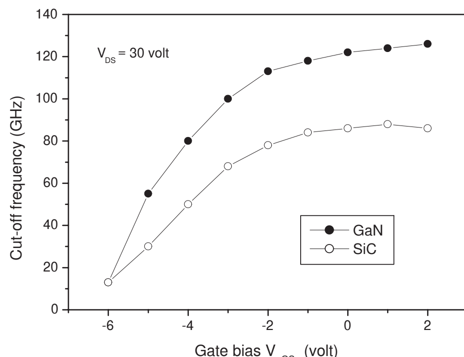

FIG. 5: Current gain cut-off frequency as a function of gate bias. Comparison of GaN and SiC MESFET.

under the gate is reduced in two ways; there is a reduction in the transit length and also the electron velocity is larger. The high value of the field at the source-end of the gate is responsible for the almost ballistic acceleration of the electrons as soon as they enter the channel region under the gate. As a result, shorter devices lead to higher cutoff frequencies but they are also expected to lead to smaller breakdown voltages.
Figures 5 and 6 present the evolution of transconductance g_m (Fig. 5) and current gain cut-off frequency f_c (Fig. 6) versus gate voltage V_{gs}, at V_{ds}=30 V, for both structures. Due to the better electronic properties and higher drain current densities, GaN MESFET exhibits 70% higher transconductance and cut-off frequency. For example, at V_{gs}=0.2 V, we obtained transconductance of 300 mS mm^{-1} and cutoff frequency of 120 GHz for the GaN MESFET, against 160 mS mm^{-1} and 85 GHz for the SiC. These results show that GaN MESFETs may perform quite well for high frequency operations as well as for high power applications.

4. CONCLUSIONS

The Monte Carlo technique has been used to compare the potentialities of GaN and SiC MESFETs. We find that both materials are good candidates for high frequency and high power operations. At low operationg frequencies GaN drain *IV* characteristics are superior to those of SiC, possessing greater output resistances and higher gains. However, the SiC devices displayed substantially greater stability with respect to changes of voltage because of the ability of SiC to maintain a positive differential resistance at the drain contact due to ballistic effects under the gate.

Acknowledgements

The author wish to thank M. G. Paeezi for helpful comments and for critical reading of the manuscript.

[1] R. Mickevicius and J. H. Zhao, *J. Appl. Phys.* **83**, 3161 (1998)
[2] R. J. Trew and M. W. Shin, *Third Int. Conf. on Integrated Nonlinear Microwave and Millimeterwave Circuits Dig.*, 109 (1994)
[3] K. Dohnke, R. Rupp, D. Peters, J. Volkl and D. Stephani, *Institute of Physics Conf. Series, IOP Publishing*, Bristol, UK, 625 (1994)
[4] A. K. Agarwal, *The Second Int. Electric Electronic Combat Vehicle Conf. AECV-II*, Dearborn, MI, (1997)
[5] R. P. Joshi, *J. Appl. Phys.* **78**, 5518 (1995)
[6] H. E. Nilsson, U. Sannemo and C. S. Petersson, *J. Appl. Phys.* **80**, 3365 (1996)
[7] W. Fawcett, A. D. Boardman and S. J. Swain, *J. Phys. Chem. Solids*, **31**, (1963)
[8] C. Jacoboni and P. Lugli, *The Monte Carlo Method for semiconductor and Device Simulation*, 1989, Springer-Verlag
[9] C. Moglestue, *Monte Carlo Simulation of Semiconductor Devices*, 1993, Chapman and Hall
[10] H. Arabshahi, *Modern Physics Letters B.* **20** 787 (2006)
[11] H. Arabshahi and M. H. Ghasemian, *Modern Physics Letters B.* **22** 1397 (2006)
[12] H. Arabshahi, M. R. Benam and B. Salahi *Modern Physics Letters B.* **21**, 1715 (2007)
[13] H. Arabshahi, *Modern Physics Letters B.* **21**, 199 (2007)
[14] M. Walmsley and R. A. Abram, *Comput. Math. Electr. Electron. Eng.* **15**, 31 (1996)
[15] J. B. Roldan, F. Gamiz, J. A. Lopez-Villanueva, and P. Cartujo, *J. Electron Matter* **26**, 203 (1997)
[16] Y. C. Yeo, T. C. Chong and M. F. Li, *J. Appl. Physics.* **83**, 1429 (1998)